

# Blinding Guidance Against Missiles Sharing Bearings-Only Measurements

ROBERT FONOD , Member, IEEE

TAL SHIMA, Senior Member, IEEE

Department of Aerospace Engineering, Technion - Israel Institute of Technology, Haifa 3200003, Israel

**A novel “blind and evade” guidance concept for an aerial target, which is exposed to a threat of two homing missiles, is presented. Each missile is assumed to measure solely its own line-of-sight (LOS) angle and share it with the other missile. Such information sharing enables the missiles to form a triangular measuring baseline relative to the target and to improve their estimation accuracy. However, if the separation angle between the two LOS vectors is small enough, the observability of such double-LOS measuring approach becomes weak. Motivated by this observation, the idea of the proposed concept is to bring the missiles on the same LOS with the target, i.e., blinding them, and then perform an appropriately timed target evasive maneuver. The target’s guidance law is derived under the assumption of perfect information and formulated as an optimal control problem. Simulation results demonstrate the potential of the proposed defense concept.**

Manuscript received November 8, 2016; revised April 26, 2017 and August 6, 2017; released for publication August 22, 2017. Date of publication August 30, 2017; date of current version February 7, 2018.

DOI. No. 10.1109/TAES.2017.2747098

Refereeing of this contribution was handled by D. Ghose.

This work was supported by the U.S. Air Force Office of Scientific Research, Air Force Materiel Command, under Grant FA9550-15-1-0429. The U.S. Government is authorized to reproduce and distribute reprints for Governmental purpose notwithstanding any copyright notation thereon.

Authors’ address: R. Fonod and T. Shima are with the Department of Aerospace Engineering, Technion - Israel Institute of Technology, Haifa 3200003, Israel, E-mail: (tal.shima@technion.ac.il). (*Corresponding author: Robert Fonod*) E-mail: (robert.fonod@technion.ac.il.)

0018-9251 © 2017 IEEE

## I. INTRODUCTION

Modern highly sophisticated missiles are able to engage and destroy a large class of aerial targets such as unmanned aerial vehicles, civil or military aircraft [1], [2]. Systems developed in the past decades to increase the target’s protection capabilities are electronic countermeasures (jammers), various kinds of decoys (e.g., chaff or flares), and target defending missiles [3]–[6]. These options might be very often too complex, heavy, and expensive. On the other hand, the target may perform an evasive maneuver, which can be either arbitrary [7] or optimally adjusted against the incoming missile. Optimal deterministic one-on-one evasive strategies against a missile employing a class of linear guidance law exist, see for instance [4], [8], [9]. In the derivation of these approaches, it was assumed that the missile has perfect information about the target. However, in realistic interception scenarios with noise corrupted measurements, perfect information about the target’s states is seldom available. Therefore, an estimation algorithm is an inevitable part of any modern missile guidance system.

Most tactical missiles are equipped with affordable infrared (IR) sensors, which allow to measure the LOS angle between the missile and target. Target-tracking and observability-enhancing guidance systems in homing missiles that use bearings-only measurements have been comprehensively studied in the past [10]–[15]. In recent years, a strategy of launching multiple missiles has been perceived as a very effective way to increase the success rate of an attack. In scenarios where multiple missiles can share their respective LOS angle measurements, the missiles’ estimation performance can be significantly improved by exploiting the triangulation structure between the missiles and the target. The advantages of such information-sharing estimation concept on the interception performance are well documented in the literature [16]. The estimation quality, however, strongly depends on the missiles’ trajectories. Regardless of the filter design methodology, a general conclusion has been drawn that if the separation angle of the respective LOS vectors is too small, the relative kinematics may become weakly observable or even unobservable. Consequently, the interception performance of such missile guidance system is limited by the estimation accuracy.

Recently, an effort has been made to enhance the estimation accuracy of the multi-LOS angle measuring concept by modulating the LOS angles in opposite directions [17], by staggering launch of the missiles [18], and by enforcing a relative intercept angle between consecutive missiles [6]. While all the works discussed earlier emphasize estimation enhancement of the cooperating missiles against a single target, in this paper, the problem is posed from the target’s perspective. Taking into account the observability issues of the multi-LOS measuring environment, the desire of the target is to shape the trajectories of the homing missiles such that their LOSs with the target coincide. When this occurs, the missile-target ranges become hard to estimate and the missiles are said to be blinded. Then, to help the target to increase its probability of survival, an appropriately timed evasion maneuver is considered.

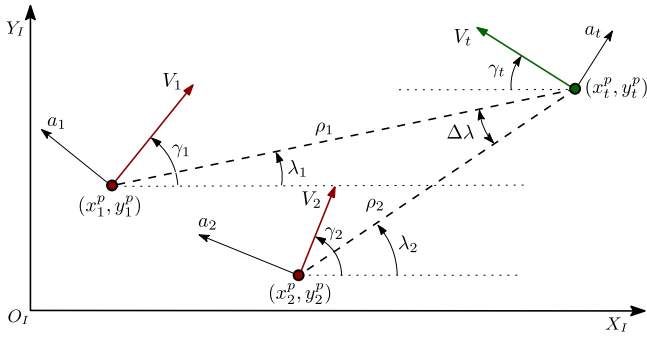


Fig. 1. Planar engagement geometry.

The proposed target's blinding-evasion guidance law is derived under the assumption of perfect information, linearized engagement model, and is formulated as an optimal control problem with a running cost on the missiles' LOS separation angle and target's control effort. It is assumed that the missiles are guided toward the target using a known linear guidance law and that they are not aware of the blinding intentions of the target. An extended Kalman filter (EKF) based cooperative target tracking estimation algorithm is proposed assuming a Singer acceleration model of the target's maneuvers. This maneuver model is discretized for the nonlinear estimation model. Using Monte Carlo (MC) simulations, the viability of the proposed blinding-evasion concept is demonstrated against attacking missiles employing classical guidance laws of proportional navigation (PN), augmented PN (APN), and optimal guidance law (OGL).

*Notations:* Bold-italic face denotes vectors and matrices;  $(\cdot)^T$  stands for transposition;  $\mathbf{0}$  represents a matrix of zeros, and  $\mathbf{I}$  an identity matrix, both with appropriate dimensions.  $\mathbb{R}^{n \times m}$  denotes a set of  $n \times m$  real matrices and  $\mathcal{N}(\mu, \sigma^2)$  denotes a Gaussian density function with mean  $\mu$  and variance  $\sigma^2$ .

## II. ENGAGEMENT

The studied engagement scenario consists of two homing missiles and an aerial target. For brevity, the attacking missiles are referred to as missiles and the aerial target as target. We consider skid-to-turn and roll-stabilized vehicles. A schematic view of the planar point mass engagement geometry is shown in Fig. 1. The Cartesian inertial reference frame is denoted by  $X_I - O_I - Y_I$ . The speed, normal acceleration, and flight-path angle are given by  $V$ ,  $a$ , and  $\gamma$ ; subscript  $i \in \{1, 2\}$  and  $t$  denotes the  $i$ th missile and the target, respectively. The pair  $(x_j^p, y_j^p)$ ,  $j \in \{1, 2, t\}$  stands for the absolute position of the  $j$ th vehicle. The range between the target and the  $i$ th missile is denoted as  $\rho_i$ . The angle between the  $i$ th missile-to-target LOS and the  $X_I$  axis is denoted as  $\lambda_i$ . The LOS separation angle  $\Delta\lambda$  will play a crucial role in the target's blinding guidance law derivation.

### A. Kinematics and Dynamics

Neglecting the gravitational force, the engagement kinematics from Fig. 1, expressed in a polar coordinate system

$(\rho_i, \lambda_i)$  attached to the  $i$ th missile, is<sup>1</sup>

$$\begin{cases} \dot{\rho}_i = V_{\rho i} \\ \dot{\lambda}_i = V_{\lambda i} / \rho_i \end{cases}, \quad i \in \{1, 2\}. \quad (1)$$

The relative velocities along ( $V_{\rho i}$ ) and normal ( $V_{\lambda i}$ ) to the LOS are

$$V_{\rho i} = -V_i \cos(\gamma_i - \lambda_i) - V_t \cos(\gamma_t + \lambda_i), \quad (2)$$

$$V_{\lambda i} = -V_i \sin(\gamma_i - \lambda_i) + V_t \sin(\gamma_t + \lambda_i). \quad (3)$$

During the endgame, all vehicles are assumed to be flying at constant speeds and to perform lateral maneuvers only. Arbitrary-order linear dynamics is assumed for all vehicles, i.e.,

$$\begin{cases} \dot{\mathbf{y}}_j = \mathbf{A}_j \mathbf{y}_j + \mathbf{B}_j u_j \\ a_j = \mathbf{C}_j \mathbf{y}_j + D_j u_j \\ \dot{\gamma}_j = a_j / V_j \end{cases}, \quad j \in \{1, 2, t\} \quad (4)$$

where  $\mathbf{y}_j \in \mathbb{R}^{n_j}$  is the internal state vector of the  $j$ th vehicle's internal dynamics,  $a_j$  and  $u_j$  are the  $j$ th entity's normal acceleration and acceleration command, respectively.

In (4), the term  $\mathbf{C}_j \mathbf{y}_j$  is denoted as  $a_{s_j}$  and represents, if it exists, the part of the acceleration with dynamics (e.g., an angle of attack generating lift). The second part of the acceleration, i.e.,  $D_j u_j$ , represents the direct lift, which can be obtained immediately from deflection of the steering mechanism such as the canard or tail.

We assume that all vehicles have maneuverability limitations defined as

$$|u_j| \leq \bar{u}_j \quad \forall j \in \{1, 2, t\} \quad (5)$$

where  $\bar{u}_j > 0$  is the  $j$ th vehicle's maximal acceleration.

### B. Timeline and Time-to-Go

The running time is denoted as  $t$ . The endgame initiates at  $t = t_0 = 0$  with  $\dot{\rho}_i(t_0) < 0$ ,  $\forall i \in \{1, 2\}$ . The  $i$ th engagement terminates at  $t = t_i^f$ , where  $t_i^f$  is the fixed interception time of the  $i$ th missile defined as

$$t_i^f \triangleq \arg \inf_{t > 0} \{\rho_i(t) V_{\rho i}(t) = 0\} \quad \forall i \in \{1, 2\}. \quad (6)$$

The interception time  $t_i^f$  allows us to define the nonnegative time-to-go  $t_i^{\text{go}}$  of the  $i$ th missile as

$$t_i^{\text{go}} \triangleq \begin{cases} t_i^f - t, & t \leq t_i^f \\ 0, & t > t_i^f \end{cases} \quad \forall i \in \{1, 2\}. \quad (7)$$

At  $t = t_i^f$ , the separation  $\rho_i(t_i^f)$  is minimal and it is referred to as "miss distance" or compactly as "miss."

Without loss of generality, it is assumed that the missiles are numbered based on their interception times satisfying

$$t_1^f \leq t_2^f. \quad (8)$$

<sup>1</sup>For notational simplicity, the reference to the independent time variable " $t$ " will be omitted whenever the context is clear.

### C. Missiles' Measurement Model

We assume that each missile is equipped with an IR sensor only and that both missiles acquire their LOS angle measurements at the same discrete-time  $t = t_k \triangleq kT$ , where  $T > 0$  is a constant measurement sampling period. Furthermore, the  $i$ th missile measurement,<sup>2</sup>  $z_{i;k}$ , is assumed to be contaminated by a zero-mean white Gaussian noise with a fixed standard deviation  $\sigma_{\lambda_i}$ . Based on the above assumptions, the physical measurement model of the  $i$ th missile at time  $t_k$  is

$$z_{i;k} = h(\mathbf{x}_{i;k}) + v_{i;k} \triangleq \lambda_{i;k} + v_{i;k}, \quad i \in \{1, 2\} \quad (9)$$

where  $\mathbf{x}_{i;k}$  is the estimated state vector (being defined later) and  $v_{i;k}$  is the measurement noise satisfying

$$v_{i;k} \sim \mathcal{N}(0, \sigma_{\lambda_i}^2).$$

The measurement noises of the missiles are assumed to be mutually independent, therefore,  $E[v_{1;k}v_{2;k}] = 0$ .

Next, we will assume that each missile can transmit its own-ship measurement to the other missile without any delay and that the relative positions between the missiles

$$\begin{cases} \tilde{x}_{ij} \triangleq x_i^p - x_j^p \\ \tilde{y}_{ij} \triangleq y_i^p - y_j^p \end{cases}, \quad i, j \in \{1, 2\} \quad (10)$$

are known accurately (e.g., using inertial navigation system and/or GPS sensors). Such an information exchange may enable the missiles to form a relative measuring baseline with respect to the target. Hence, if target tracking and estimation is performed using measurements from both missiles, the measurement model of the  $i$ th missile becomes

$$\mathbf{z}_k \triangleq \begin{bmatrix} z_{1;k} \\ z_{2;k} \end{bmatrix} = \mathbf{h}_{i;k}(\mathbf{x}_{i;k}) + \mathbf{v}_k \quad (11)$$

where  $\mathbf{h}_{i;k} \triangleq [h_{i;k}^1(\mathbf{x}_{i;k}) \ h_{i;k}^2(\mathbf{x}_{i;k})]^T$  and  $\mathbf{v}_k \triangleq [v_{1;k} \ v_{2;k}]^T$ .

In (11), the measurement from the  $j$ th missile is expressed using the  $i$ th missile relative states as ( $j \neq i$ )

$$h_{i;k}^j(\mathbf{x}_{i;k}) = \tan^{-1} \left( \frac{\tilde{y}_{ij;k} + \rho_{i;k} \sin(\lambda_{i;k})}{\tilde{x}_{ij;k} + \rho_{i;k} \cos(\lambda_{i;k})} \right) \quad (12)$$

where  $\tilde{x}_{ij;k}$  and  $\tilde{y}_{ij;k}$  are the relative positions (10) taken from the  $k$ th time frame. For  $j = i$ ,  $h_{i;k}^j(\mathbf{x}_{i;k})$  degenerates to  $h(\mathbf{x}_{i;k})$  defined in (9).

We assume that if the  $i$ th missile passes the target ( $t_i^{\text{go}} = 0$ ), then it stops transmitting measurements to the other missile.

### III. ESTIMATOR DESIGN FOR THE MISSILES

To implement a homing guidance law in realistic scenarios, some variables must be estimated from the available noise-corrupted measurements. Therefore, in this section, we incorporate a relatively simple measurements-sharing

<sup>2</sup>Hereafter, the subscript  $k$ , separated by a semicolon, will denote the discrete-time  $t_k$ .

target tracking estimator in order to demonstrate the estimation effect on the homing accuracy of the missiles.<sup>3</sup>

#### A. Target Maneuver Model

To model the target maneuvers, we consider the Singer acceleration model [19]. This model represents the correlation function  $r(\tau)$  of the target acceleration  $a_t(t)$  to be a scalar stochastic process with exponentially decaying autocorrelation

$$r(\tau) = \sigma_t^2 e^{-\alpha|\tau|} \quad (13)$$

where  $\sigma_t^2$  is the instantaneous variance of the target acceleration and  $\alpha > 0$  is the reciprocal of the time constant of the target acceleration autocorrelation [20]. For example,  $\alpha \simeq 1/60$  for a lazy turn,  $\alpha \simeq 1/20$  for an evasive maneuver, and  $\alpha \simeq 1$  for atmospheric turbulence [19]. Singer [19] suggested to choose  $\sigma_t^2$  as follows

$$\sigma_t^2 = \bar{u}_t^2(1 + 4P_{\max} - P_0)/3 \quad (14)$$

where  $P_{\max}$  is the probability of the target accelerating at  $\pm \bar{u}_t$  and  $P_0$  is the probability of the target not maneuvering.

The state equation corresponding to (13) is

$$\dot{a}_t(t) = -\alpha a_t(t) + \tilde{w}(t) \quad (15)$$

where  $\tilde{w}(t)$  is a zero-mean white Gaussian process with the following autocorrelation function

$$E[\tilde{w}(t + \tau)\tilde{w}(t)] = 2\alpha\sigma_t^2\delta(\tau) \quad (16)$$

where  $\delta(\tau)$  is the Dirac delta function.

#### B. Estimation Model

Assume that missile-related parameters such as  $y_i$ ,  $\gamma_i$ , and  $V_i$  are known accurately. Most guidance laws are implemented in relative polar coordinates  $(\rho_i, \lambda_i)$ , see for example, the classical guidance laws in Appendix A. Therefore, we define the state vector of the target for the  $i$ th missile estimator in such a coordinate system, i.e.,

$$\mathbf{x}_i \triangleq [\rho_i \ \lambda_i \ \gamma_t \ a_t \ V_t]^T, \quad i \in \{1, 2\}. \quad (17)$$

Using the Singer model (15), the equations of motion (EOM) for the  $i$ th estimator design become

$$\dot{\mathbf{x}}_i = \mathbf{f}_i(\mathbf{x}_i) \triangleq \begin{bmatrix} V_{\rho_i} \\ V_{\lambda_i}/\rho_i \\ a_t/V_t \\ -\alpha a_t + \tilde{w} \\ 0 \end{bmatrix} \quad (18)$$

where  $V_{\rho_i}$  and  $V_{\lambda_i}$  are given in (2) and (3), respectively.

The discrete-time version of (18) can be compactly written as

$$\mathbf{x}_{i;k} = \mathbf{f}_{i;k-1}(\mathbf{x}_{i;k-1}) + \mathbf{w}_{i;k} \quad (19)$$

where  $\mathbf{x}_{i;k}$  is the state vector of the  $i$ th missile at time  $t_k$ ,  $\mathbf{f}_{i;k-1}$  is a vector function obtained by integrating (18)

<sup>3</sup>Clearly, another estimation scheme or target maneuver model could be considered, although we expect a similar trend in the estimation effects.

from  $t_{k-1}$  to  $t_k$  with  $\tilde{w} = 0$ . In (19),  $\mathbf{w}_{i;k}$  is a vector valued zero-mean white noise sequence, which relates to the scalar continuous-time process  $\tilde{w}$  as follows

$$\mathbf{w}_{i;k} = \int_{t_{k-1}}^{t_k} e^{(t_k-\tau)\mathbf{F}_{i;k}} \mathbf{G} \tilde{w}(\tau) d\tau \quad (20)$$

where  $\mathbf{G} = [0 \ 0 \ 0 \ 1 \ 0]^T$  and  $\mathbf{F}_{i;k}$  is the Jacobian matrix associated with (18) and evaluated at  $\mathbf{x} = \mathbf{x}_{i;k-1}$ , i.e.,

$$\mathbf{F}_{i;k} \triangleq \left. \frac{\partial \mathbf{f}_i(\mathbf{x})}{\partial \mathbf{x}} \right|_{\mathbf{x}=\mathbf{x}_{i;k-1}}. \quad (21)$$

It is assumed that  $\mathbf{F}_{i;k}$  is fixed during the time interval  $(t_{k-1}, t_k)$ . Denote  $\sin(\gamma_t + \lambda_i)$  by  $s_i$  and  $\cos(\gamma_t + \lambda_i)$  by  $c_i$ , then

$$\frac{\partial \mathbf{f}_i(\mathbf{x})}{\partial \mathbf{x}} = \begin{bmatrix} 0 & V_{\lambda i} & s_i V_t & 0 & -c_i \\ -V_{\lambda i} \rho_i^{-2} & -V_{\rho i} \rho_i^{-1} & c_i V_t \rho_i^{-1} & 0 & s_i \rho_i^{-1} \\ 0 & 0 & 0 & V_t^{-1} & -a_t V_t^{-2} \\ 0 & 0 & 0 & -\alpha & 0 \\ 0 & 0 & 0 & 0 & 0 \end{bmatrix}.$$

With the zero-mean and white assumption on  $\tilde{w}(t)$ , it follows that

$$E[\mathbf{w}_{i;k}] = \mathbf{0}, \quad E[\mathbf{w}_{i;k} \mathbf{w}_{i;l}^T] = \mathbf{Q}_{i;k}^w \delta_{kl} \quad (22)$$

where  $\delta_{kl}$  stands for the Kronecker delta function and  $\mathbf{Q}_{i;k}^w$  is the covariance matrix of  $\mathbf{w}_{i;k}$ , satisfying

$$\mathbf{Q}_{i;k}^w = 2\alpha \sigma_t^2 \int_{t_{k-1}}^{t_k} e^{(t_k-\tau)\mathbf{F}_{i;k}} \mathbf{G} \mathbf{G}^T e^{(t_k-\tau)\mathbf{F}_{i;k}^T} d\tau. \quad (23)$$

Using the first-order Taylor series approximation of  $e^{(t_k-\tau)\mathbf{F}_{i;k}}$ , the above integral can be easily solved. Consequently,  $\mathbf{Q}_{i;k}^w$  can be approximated as

$$\mathbf{Q}_{i;k}^w \approx 2T\alpha \sigma_t^2 \left[ \mathbf{G} \mathbf{G}^T + \frac{T}{2} \tilde{\mathbf{G}}_{i;k} + \frac{T^2}{3} \mathbf{F}_{i;k} \mathbf{G} \mathbf{G}^T \mathbf{F}_{i;k}^T \right] \quad (24)$$

where  $T = t_k - t_{k-1}$  and  $\tilde{\mathbf{G}}_{i;k} = \mathbf{F}_{i;k} \mathbf{G} \mathbf{G}^T + \mathbf{G} \mathbf{G}^T \mathbf{F}_{i;k}^T$ .

### C. Extended Kalman Filter

The estimation model (18) is nonlinear, thus an EKF is used to estimate  $\mathbf{x}_{i;k}$  for the  $i$ th missile.

1) *Time Propagation*: The state estimate of the  $i$ th missile's filter at time  $t_k$  using measurements up to time  $t_{k-1}$ ,  $\hat{\mathbf{x}}_{i;k-1|k-1}$ , is propagated from  $t_{k-1}$  to  $t_k$  using (18) with  $\mathbf{w}_{i;k} = \mathbf{0}$ . The prediction error covariance matrix is propagated as

$$\mathbf{P}_{i;k|k-1} = \Phi_{i;k} \mathbf{P}_{i;k-1|k-1} \Phi_{i;k}^T + \mathbf{Q}_{i;k}^w \quad (25)$$

where  $\Phi_{i;k} \triangleq \exp(T\mathbf{F}_{i;k})$  is the state transition matrix,  $\mathbf{F}_{i;k}$  is the state Jacobian matrix (21) evaluated at  $\mathbf{x} = \hat{\mathbf{x}}_{i;k-1|k-1}$ , and  $\mathbf{Q}_{i;k}^w$  is given in (24).

2) *Measurement Update*: This stage depends on whether the measurements have been exchanged or not.

For the case when both measurements are available, the predicted state estimate  $\hat{\mathbf{x}}_{i;k|k-1}$  is updated as

$$\hat{\mathbf{x}}_{i;k|k} = \hat{\mathbf{x}}_{i;k|k-1} + \mathbf{K}_{i;k} (\mathbf{z}_k - \mathbf{h}_{i;k}(\hat{\mathbf{x}}_{i;k|k-1})) \quad (26)$$

where  $\mathbf{K}_{i;k}$  is the Kalman gain matrix given by

$$\mathbf{K}_{i;k} = \mathbf{P}_{i;k|k-1} \mathbf{H}_{i;k}^T (\mathbf{H}_{i;k} \mathbf{P}_{i;k|k-1} \mathbf{H}_{i;k}^T + \mathbf{R}^v)^{-1}. \quad (27)$$

Here,  $\mathbf{R}^v = \text{diag}\{\sigma_{\lambda 1}^2, \sigma_{\lambda 2}^2\}$  is the covariance matrix of  $\mathbf{v}_k$  and

$$\mathbf{H}_{i;k} \triangleq \left. \frac{\partial \mathbf{h}_{i;k}(\mathbf{x})}{\partial \mathbf{x}} \right|_{\mathbf{x}=\hat{\mathbf{x}}_{i;k|k-1}} = \begin{bmatrix} H_{i;k}^{\rho 1} & H_{i;k}^{\lambda 1} & 0 & 0 & 0 \\ H_{i;k}^{\rho 2} & H_{i;k}^{\lambda 2} & 0 & 0 & 0 \end{bmatrix} \Bigg|_{\mathbf{x}=\hat{\mathbf{x}}_{i;k|k-1}} \quad (28)$$

is the measurement Jacobian matrix derived from (11). The scalar parameters  $H_{i;k}^{\rho j}$  and  $H_{i;k}^{\lambda j}$  are given by

$$H_{i;k}^{\rho j} = \frac{\tilde{x}_{ij} \sin(\lambda_i) - \tilde{y}_{ij} \cos(\lambda_i)}{\tilde{x}_{ij}^2 + \tilde{y}_{ij}^2 + \rho_i^2 + 2\rho_i (\tilde{x}_{ij} \cos(\lambda_i) + \tilde{y}_{ij} \sin(\lambda_i))}$$

$$H_{i;k}^{\lambda j} = \frac{(\tilde{x}_{ij} \cos(\lambda_i) + \tilde{y}_{ij} \sin(\lambda_i) + \rho_i) \rho_i}{\tilde{x}_{ij}^2 + \tilde{y}_{ij}^2 + \rho_i^2 + 2\rho_i (\tilde{x}_{ij} \cos(\lambda_i) + \tilde{y}_{ij} \sin(\lambda_i))}.$$

In (28),  $\rho_i$  and  $\lambda_i$  are substituted with the appropriate values from the estimated state vector  $\hat{\mathbf{x}}_{i;k|k-1}$ . The missiles' relative positions  $\tilde{x}_{ij}$  and  $\tilde{y}_{ij}$  are considered from the  $k$ th time frame. Finally, the estimation error covariance matrix is updated via

$$\mathbf{P}_{i;k|k} = \mathbf{P}_{i;k|k-1} - \mathbf{K}_{i;k} \mathbf{H}_{i;k} \mathbf{P}_{i;k|k-1}. \quad (29)$$

If the measurements have not been exchanged (e.g., because one of the missiles ceased to exist, or due to sensor error or blind range of the sensor), then the measurement update stage of the  $i$ th missile estimator is performed using the own-ship measurement ( $\mathbf{z}_{i;k}$ ) only. In this case, the measurement Jacobian matrix and measurement noise covariance matrix degenerate to

$$\mathbf{H}_{i;k} = [0 \ 1 \ 0 \ 0 \ 0], \quad \mathbf{R}^v = [\sigma_i^2] \quad (30)$$

and  $\mathbf{h}_{i;k}(\hat{\mathbf{x}}_{i;k|k-1})$  in (26) is replaced by (9).

REMARK 1 In this paper, we assume that estimation is always performed using shared measurements unless one of the missile's ceases to exist.

### D. Observability Analysis

The range between the target and the  $i$ th missile, i.e.,  $\rho_i$ , can be related to the noisy LOS measurements of the  $i$ th and the  $j$ th missile and to their relative position ( $\rho_{ij}, \lambda_{ij}$ ) as follows

$$\rho_{i;k}^\dagger = \rho_{i;j;k} \frac{\sin(\lambda_{i;j;k} - z_{j;k})}{\sin(z_{i;k} - z_{j;k})}, \quad i \neq j \quad (31)$$

where

$$\rho_{i;j;k} = \sqrt{\tilde{x}_{ij;k}^2 + \tilde{y}_{ij;k}^2}, \quad \lambda_{i;j;k} = \tan^{-1} \left( \frac{\tilde{y}_{ij;k}}{\tilde{x}_{ij;k}} \right).$$

The range  $\rho_{i;k}^\dagger$  can be viewed as a pseudomeasurement of  $\rho_i$  at time  $t_k$ . Using (9) in (31), it is easy to show that  $\rho_{i;k}^\dagger$  is distributed according to [17]

$$\rho_{i;k}^\dagger \sim \mathcal{N}(\rho_{i;k}, \sigma_{\rho_{i;k}}^2) \quad (32)$$

where  $\rho_{i;k}$  is the true range at time  $t_k$  and  $\sigma_{\rho_{i;k}}$  is the nonstationary standard deviation of  $\rho_{i;k}^\dagger$ , given by (the subscript  $k$  is omitted to avoid excessive indexing)

$$\sigma_{\rho_i} = \rho_{ij} \times \frac{\sqrt{\sigma_j^2 \sin^2(\lambda_{ij} - \lambda_i) + \sigma_i^2 \sin^2(\lambda_{ij} - \lambda_j) \cos^2(\lambda_i - \lambda_j)}}{\sin^2(\lambda_i - \lambda_j)}.$$

Letting  $|\lambda_i - \lambda_j| \rightarrow 0$  in the above expression yields

$$\lim_{|\lambda_i - \lambda_j| \rightarrow 0} \sigma_{\rho_i} = \infty, \quad i \neq j, \rho_{ij} \neq 0. \quad (33)$$

This limit holds also when  $|\lambda_{ij} - \lambda_l| \rightarrow 0, l \in \{i, j\}$ .

From (33), it can be concluded that if the difference between the two LOS angles  $\lambda_1$  and  $\lambda_2$  becomes very small (close to zero), the variance of the pseudomeasurement  $\rho_{i;k}^\dagger$  increases, which in turn shall make the range of the  $i$ th missile unobservable from the other missile perspective. In other words, the shared measurements will contain the same information as the measurement of the either missile.

#### IV. TARGET'S BLINDING-EVASION GUIDANCE

Based on the discussion in the previous section, the observability of the double-LOS measuring scheme may become weak when  $|\lambda_2 - \lambda_1|$  is small enough. Define the difference between these two angles as

$$\Delta\lambda \triangleq \lambda_2 - \lambda_1. \quad (34)$$

This difference will be referred to as the *LOS separation angle*.

If  $\Delta\lambda \rightarrow 0$  (i.e., both missiles are on the same LOS with the target), then the range becomes weakly observable and we say that the ‘‘missiles are blinded.’’ This is expected to lead to a significant deterioration of the missiles’ estimation accuracy, especially of the range, target’s speed, and time-to-go estimates. As a consequence, poor estimation performance may lead to poor homing accuracy of the missiles.

In this section, we aim at developing a guidance strategy for the target that will minimize  $|\Delta\lambda|$  and will perform an evasive maneuver once the missiles are blinded.

##### A. Linearized Kinematics for Guidance Law Derivation

We will perform the derivation of the target’s blinding guidance law based on a linearized model. If during the endgame the missiles and target deviations from the respective collision triangles are small, then linearization is justified [21].

Fig. 2 shows a schematic view of the linearized planar engagement geometry of the  $i$ th missile and the target. The  $X_i$  axis aligned with the LOS used for linearization is denoted as  $\text{LOS}_{i;0}$ . The relative displacement between

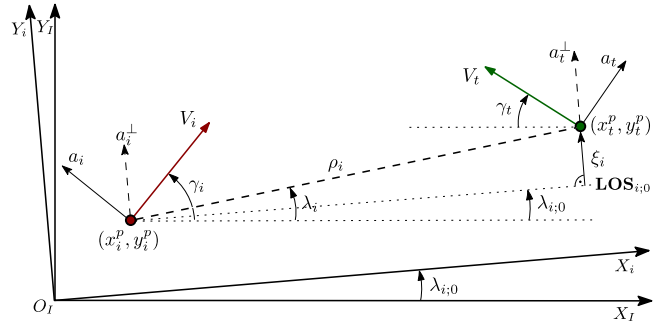


Fig. 2. Linearized planar engagement geometry.

the target and the  $i$ th missile normal to this direction is  $\xi_i$ . The acceleration of the  $i$ th missile and the target normal to  $\text{LOS}_{i;0}$  is denoted by  $a_i^\perp$  and  $a_t^\perp$ , respectively, and satisfy

$$a_i^\perp = k_i a_i, \quad k_i = \cos(\gamma_{i;0} - \lambda_{i;0}) \quad (35)$$

$$a_t^\perp = k_t a_t, \quad k_t = \cos(\gamma_{t;0} + \lambda_{i;0}) \quad (36)$$

where  $k_i$  and  $k_t$  are the linearization parameters of the  $i$ th engagement. The subscript ‘‘0’’ denotes the initial value around which the linearization has been performed.

The LOS separation angle  $\Delta\lambda$  was defined in (34) using the LOS angles that relate to the nonlinear model given in (1). Suppose that  $|\lambda_{2;0} - \lambda_{1;0}|$  is sufficiently small, then  $\Delta\lambda$  can be approximated as

$$\Delta\lambda \approx \sin(\lambda_2 - \lambda_{2;0}) - \sin(\lambda_1 - \lambda_{1;0}) \triangleq x_\lambda. \quad (37)$$

From Fig. 2,  $x_\lambda$  can be expressed using the linearized variables  $\xi_1$  and  $\xi_2$  as follows

$$x_\lambda = \xi_2/\rho_2 - \xi_1/\rho_1. \quad (38)$$

Based on the constant speeds and linearization assumptions, the  $i$ th range  $\rho_i$  can be approximated as

$$\rho_i \approx V_{ci} t_i^{\text{go}} \quad (39)$$

where

$$V_{ci} = V_i k_i + V_t k_t$$

is the constant closing speed of the  $i$ th engagement. Differentiating (38) with respect to time and using (39) yields

$$\dot{x}_\lambda = \frac{\dot{\xi}_2}{V_{c2} t_2^{\text{go}}} + \frac{\xi_2}{V_{c2} (t_2^{\text{go}})^2} - \frac{\dot{\xi}_1}{V_{c1} t_1^{\text{go}}} - \frac{\xi_1}{V_{c1} (t_1^{\text{go}})^2}. \quad (40)$$

Let the missiles’ internal states and controls be gathered in the following vectors

$$\mathbf{y}_m \triangleq [\mathbf{y}_1^T \quad \mathbf{y}_2^T]^T, \quad \mathbf{u}_m \triangleq [u_1 \quad u_2]^T.$$

Now, define the state vector of the linearized blinding guidance problem as

$$\mathbf{x} \triangleq [\mathbf{x}_\xi^T \quad \mathbf{x}_{d\xi}^T \quad \mathbf{y}_m^T \quad \mathbf{y}_t^T \quad x_\lambda]^T \quad (41)$$

where  $\mathbf{x}_\xi$  is a vector of the two relative displacements, i.e.,

$$\mathbf{x}_\xi = [\xi_1 \quad \xi_2]^T \triangleq [x_1 \quad x_2]^T$$

and  $\mathbf{x}_{d\xi}$  is its derivative, i.e., a vector of relative speeds normal to the respective initial LOSs.

The EOM associated with the state vector (41) are

$$\begin{cases} \dot{x}_1 = x_3 \\ \dot{x}_2 = x_4 \\ \dot{x}_3 = k_{t_1} a_t - k_1 a_1 \\ \dot{x}_4 = k_{t_2} a_t - k_2 a_2 \\ \dot{\mathbf{y}}_m = \mathbf{A}_m \mathbf{y}_m + \mathbf{B}_m \mathbf{u}_m \\ \dot{\mathbf{y}}_t = \mathbf{A}_t \mathbf{y}_t + \mathbf{B}_t \mathbf{u}_t \\ \dot{x}_\lambda = -\frac{x_1}{V_{c1}(t_1^{\text{go}})^2} + \frac{x_2}{V_{c2}(t_2^{\text{go}})^2} - \frac{x_3}{V_{c1} t_1^{\text{go}}} + \frac{x_4}{V_{c2} t_2^{\text{go}}} \end{cases} \quad (42)$$

where  $\mathbf{A}_m$  and  $\mathbf{B}_m$  are block diagonal matrices defined as:  $\mathbf{A}_m \triangleq \text{diag}\{\mathbf{A}_1, \mathbf{A}_2\}$  and  $\mathbf{B}_m \triangleq \text{diag}\{\mathbf{B}_1, \mathbf{B}_2\}$ .

We assume that the guidance law of the  $i$ th missile can be represented in the following linear form [21]

$$u_i = K_i^1 \xi_i + K_i^2 \dot{\xi}_i + \mathbf{K}_i^m \mathbf{y}_i + \mathbf{K}_i^t \mathbf{y}_t + K_i^u u_t \quad (43)$$

where each parameter can be, in general, a function of  $t_i^{\text{go}}$ . This representation allows us to consider a large class of linear guidance laws, commonly derived under the assumption of linear kinematics, perfect information, and unbounded controls. The well-known classical guidance laws of PN, APN, and OGL can also be represented in the form of (43), see Appendix A.

Finally, using (43), we can write the matrix form of the linearized equation set (42) as

$$\dot{\mathbf{x}}(t) = \mathbf{A}(t)\mathbf{x}(t) + \mathbf{B}(t)u_t(t), \quad \mathbf{x}(0) = \mathbf{x}_0 \quad (44)$$

where

$$\mathbf{A}(t) = \begin{bmatrix} \mathbf{0} & \mathbf{I} & \mathbf{0} & \mathbf{0} & 0 \\ A_{21}^\circ & A_{22}^\circ & A_{23}^\circ & A_{24}^\circ & 0 \\ A_{31}^\circ & A_{32}^\circ & A_{33}^\circ & A_{34}^\circ & 0 \\ \mathbf{0} & \mathbf{0} & \mathbf{0} & \mathbf{A}_t & 0 \\ A_{51}^\circ & A_{52}^\circ & \mathbf{0} & \mathbf{0} & 0 \end{bmatrix}, \quad \mathbf{B}(t) = \begin{bmatrix} \mathbf{0} \\ \mathbf{B}_2^\circ \\ \mathbf{B}_3^\circ \\ \mathbf{B}_t \\ 0 \end{bmatrix}.$$

The matrices  $\mathbf{A}^\circ$  and  $\mathbf{B}^\circ$  are given in Appendix B. Note that both  $\mathbf{A}$  and  $\mathbf{B}$  are in general functions of the independent time  $t$ , see the definition of  $t_i^{\text{go}}$  in (7).

**REMARK 2** The assumption that  $u_i$  may be dependent on  $u_t$  arises from the fact that if the missile uses an optimal-control-based guidance law, then the underlying assumption in its derivation was that the target's controller is known not just at the current time but also from the current time until the end of the scenario [4].

## B. Optimal Blinding Controller

Define the interception time of the shortest engagement as<sup>4</sup>

$$t^f \triangleq \min_{i \in \{1,2\}} t_i^f. \quad (45)$$

We chose a quadratic cost function  $J$ , which combines minimization of the LOS separation angle  $x_\lambda$  and minimiza-

tion of the target's control effort  $u_t$ , as follows

$$J = \frac{1}{2} \int_{t_0}^{t_s^f} [Q(\tau)x_\lambda^2(\tau) + R u_t^2(\tau)] d\tau \quad (46)$$

where  $t_s^f \leq t^f$  is a fixed blinding time (duration) being specified later,  $R > 0$  is a constant weight on the target's control effort, and

$$Q(\tau) \triangleq \frac{\eta}{t_s^f - \tau} \quad (47)$$

is a time dependent weighting factor on the approximate LOS separation angle with  $\eta \geq 0$ .

Suppose that  $x_\lambda$  is completely controllable on the closed interval  $t \in \langle 0, t_s^f \rangle$  by the target's control  $u_t$  [22], then the optimal state-feedback solution that minimizes the above cost function subject to the system dynamics (44) is given by [23]

$$u_t^*(t) = -R^{-1} \mathbf{B}^T(t) \mathbf{P}(t) \mathbf{x}(t), \quad t \in \langle 0, t_s^f \rangle \quad (48)$$

where  $u_t^*$  is the target's optimal controller and  $\mathbf{P} = \mathbf{P}^T \geq \mathbf{0}$  satisfies the differential matrix Riccati equation

$$\dot{\mathbf{P}} = -\mathbf{A}^T \mathbf{P} - \mathbf{P} \mathbf{A} + \mathbf{P} \mathbf{B} R^{-1} \mathbf{B}^T \mathbf{P} - \mathbf{C}^T \mathbf{Q} \mathbf{C} \quad (49)$$

with boundary condition  $\mathbf{P}(t_s^f) = \mathbf{0}$ . In (49),  $\mathbf{C}$  is a constant row vector that pulls out  $x_\lambda$  from the state vector  $\mathbf{x}$  defined in (41). The above Riccati equation must be solved backward in time, i.e., from the terminal time  $t = t_s^f$  to the initial time  $t = 0$ . Because a closed-form solution for  $\mathbf{P}$  is a nontrivial problem, it will be computed numerically.

Note that if  $\eta > 0$ , the weighting factor  $Q(\tau)$  will approach infinity as  $\tau \rightarrow t_s^f$ . Such weighting of the LOS separation angle is desirable as it stresses the importance of the blinding toward the end of the blinding phase ( $t \rightarrow t_s^f$ ). Letting  $\eta \rightarrow \infty$  enforces quicker convergence of  $\Delta\lambda$  to zero. Similarly,  $R \rightarrow \infty$  leads to a nonmaneuvering target.

**REMARK 3** The guidance law of (48) is formulated under the assumption that the guidance laws and parameters of the missiles are perfectly known to the target. Although, this assumption seems at first very limiting, it has been shown in [3] and [8] that if a missile's guidance law belongs to a known set of guidance laws, then its guidance law, guidance parameters, and states can be very accurately estimated.

## C. Blind and Evade Strategy

Employing a pure blinding guidance strategy throughout the entire engagement might be risky as the missiles, even when properly blinded, might be on the right collision course and may hit the target. Therefore, the blinding duration  $t_s^f$  shall be defined as

$$t_s^f \triangleq t^f - \Delta t_s \quad (50)$$

where  $0 < \Delta t_s < t^f$ . The value of  $\Delta t_s$  determines the timing of the switch from blinding to evasion strategy.

If a missile employs a linear guidance law of the form as in (43), the resulting optimal one-on-one evasion strategy

<sup>4</sup>The rationale for defining  $t^f$  as in (45) (instead of  $t^f \triangleq t_1^f$ ) is explained in Section IV-D.

has a bang–bang structure [4]. Similarly, the optimal evasion against two missiles employing the same PN guidance law has a bang–bang structure [24]. However, to best of our knowledge, an optimal evasion strategy from two missiles, employing arbitrary guidance laws that can be written in the general linear form of (43), is still lacking in the open literature. Therefore, a clear guidance for the choice of the optimal target evasion strategy against two homing missiles, employing possible different guidance laws of the form as in (43), is missing.

In this paper, after the blinding phase terminates, we suggest the target to perform a maximum acceleration maneuver to the opposite sign of the last executed blinding command, i.e., the evasion strategy for  $t > t_s^f$  is defined as

$$u_i^e(t) = \begin{cases} +\bar{u}_i, & \text{if } u_i^*(t_s^f) \leq 0 \\ -\bar{u}_i, & \text{otherwise} \end{cases} \quad (51)$$

where  $u_i^*(t_s^f)$  is the target's control command (48) at  $t = t_s^f$ .

Finally, the proposed “blind and evade” guidance strategy for the target boils down to

$$u_i(t) = \begin{cases} u_i^*(t), & \text{if } 0 \leq t \leq t_s^f \\ u_i^e(t), & \text{otherwise} \end{cases} \quad (52)$$

where  $u_i^*$  is the blinding and  $u_i^e$  the evasion strategy given in (48) and (51), respectively.

**REMARK 4** The proposed evasion strategy (51) does not guarantee that the missiles remain blinded during the evasion phase. Nevertheless,  $\Delta t_s$  shall be chosen sufficiently small to allow proper blinding, especially when the target maneuverability is limited. Small  $\Delta t_s$  also means little time for the missiles to adapt to the abrupt change of the target's evasion maneuver and, more importantly, little time to improve their estimation accuracy, which at best (from the target perspective) might have already been significantly deteriorated due to the employed blinding guidance law.

#### D. Implementation Issues

If during the endgame the deviations from the collision triangles are small, then the linearization assumption in the derivation of the target's blinding guidance law is justified. However, if the collision geometry changes significantly throughout the engagement, then the EOM given in (44) shall be re-linearized. Subsequently, the associated Riccati equation needs to be re-solved for the updated linearization parameters

$$k_i = \cos(\gamma_{i;k} - \lambda_{i;k}), \quad k_{ti} = \cos(\gamma_{i;k} + \lambda_{i;k}). \quad (53)$$

Obviously, this might result in heavy computational burden. A way to tackle this problem is to solve the Riccati equation (49) using a fixed-step numerical integration method, e.g., using the fourth-order Runge–Kutta (RK4) algorithm [25]. Then, the solution to (49) can be obtained using a constant number of integration steps from  $t_k$  to  $t_s^f$ , where  $t_k$  is the time when re-linearization is performed. Consequently, the computation complexity at each re-linearization is equal and the integration resolution improves as the missiles approach the

end of the blinding phase. Note also that  $|\lambda_i - \lambda_{i;0}|$ , introduced in (37), can be kept arbitrarily small by proper choice of a constant update rate  $T_r > 0$  for the re-linearization procedure. This rate shall be selected by the designer to account for the available computational resources.

As discussed earlier, if  $\eta$  is nonzero, then  $Q(\tau)$  will approach infinity as  $\tau \rightarrow t_s^f$ . Obviously this might lead to numerical difficulties when attempting to solve (49) backward from  $\mathbf{P}(t_s^f) = \mathbf{0}$ . To account for this issue, the weight  $Q(\tau)$ , defined in (47), shall be approximated by

$$Q(\tau) \approx \frac{\eta}{t_s^f - \tau + \varepsilon} \quad (54)$$

where  $\varepsilon > 0$  is a sufficiently small constant selected by the designer.

Similarly, the fixed interception time assumption does not always hold in practice due to propulsion system variability, drag effects due to differences in angles of attack, etc. Therefore, the predicted interception times  $t_{i;k}^f$  need to be re-computed at each re-linearization step  $t_k$  as

$$t_{i;k}^f = \begin{cases} -\rho_{i;k}/V_{\rho i;k}, & V_{\rho i;k} < 0 \\ 0, & V_{\rho i;k} \geq 0 \end{cases} \quad (55)$$

where  $V_{\rho i;k}$  is given in (2). Due to the same reason above, the ordering of the interception times in (8) might also change. Therefore, it is necessary to update the blinding time  $t_s^f$ , defined in (50), using the most up-to-date value of  $t^f = t_k^f = \min\{t_{1;k}^f, t_{2;k}^f\}$ .

If re-linearization is performed at step  $t_k$ , then the variables  $\xi_i$  and  $\dot{\xi}_i$  can be expressed using the kinematic variables as

$$\xi_{i;k} = \rho_{i;k} \sin(\lambda_{i;k}) \quad (56)$$

$$\dot{\xi}_{i;k} = V_{\rho i;k} \sin(\lambda_{i;k}) + V_{\lambda i;k} \cos(\lambda_{i;k}) \quad (57)$$

where  $V_{\rho i}$  and  $V_{\lambda i}$  are given in (2) and (3), respectively.

**REMARK 5** While the proposed blinding concept can be easily extended to a general case of  $N$  missiles, the  $N > 2$  case requires  $N - 1$  consecutive LOS separation angles being simultaneously minimized by a single target. This may result in unrealistically high demands on the target's maneuverability to perform effective blinding or even render the blinding against  $N > 2$  missiles infeasible.

#### V. PERFORMANCE ANALYSIS

In this section, using numerical simulations, we analyze the proposed blinding–evasion concept for a team of two missiles in ballistic missile defense (BMD) scenario. Different values of the switch parameter  $\Delta t_s$  and the target's maneuverability limit  $\bar{u}_i$  are considered to evaluate the pure estimation performance as well as the intertwined guidance–estimation performance of the missiles.

##### A. Interception Scenario and Parameters

The BMD example considered in this paper is partially based on the example introduced in [18]. For all simulations, the missiles are launched simultaneously at the

beginning of the engagement. The initial horizontal separation between the target and missiles is 15 km. The missiles are initiated at a vertical separation of  $\tilde{y}_{12} = -\tilde{y}_{21} = 100$  m and the target in the positive  $X_I$  direction from the missiles. All vehicles are flying with the same constant speed  $V_1 = V_2 = V_t = 2500$  m/s and have first-order lateral dynamics with time constants  $\tau_1 = \tau_2 = 0.1$  s, and  $\tau_t = 0.2$  s. Thus, matrices in (4) degenerate to  $A_i = -1/\tau_i$ ,  $B_i = 1/\tau_i$ ,  $C_i = 1$ , and  $D_i = 0$ ,  $i \in \{1, 2, t\}$ . The derivation of the target's blinding guidance law was performed assuming unbounded controls. However, for the sake of practicality, we limit the target maneuverability to  $\bar{u}_t \in \mathcal{G}_t \triangleq \{5, 10, 15, 20\}g$ , where  $g = 9.80665$  m/s<sup>2</sup> is the acceleration due to the gravity. The maximal maneuverability of the missiles is  $\bar{u}_1 = \bar{u}_2 = 45g$ .

The missiles are guided toward the target via one of the classical guidance laws of PN, APN, or OGL, see Appendix A. The estimator developed in Section III is implemented for each missile at the sampling rate of 100 Hz ( $T = 0.01$  s). The simulated measurement noises are with  $\sigma_1 = \sigma_2 = 0.5$  mrad. The Singer model parameters are set to  $\alpha = 1/\tau_t$  and  $\sigma_t = \bar{u}_t$ . This choice corresponds to  $P_{\max} = 1/3$  and  $P_0 = 2/3$  in (14). For MC simulations, the initial state of the  $i$ th filter is sampled as

$$\hat{x}_{i;0|0} \sim \mathcal{N}(x_{i;0}, P_{i;0|0})$$

where  $x_{i;0}$  is the true initial state vector defined in (17) and  $P_{i;0|0}$  is the initial covariance matrix of the error being set as

$$P_{i;0|0} = \text{diag}\{50^2 (\pi/180)^2 (3\pi/180)^2 (1g)^2 100^2\}.$$

The parameters of the blinding guidance law are set to  $R = 1$ ,  $\eta = 10^{11}$ , and  $\varepsilon = 10^{-8}$ . The target's control (52) is implemented at a rate of 100 Hz. The EOM for the blinding problem are re-linearized at the same rate, i.e.,  $T_r = 0.01$  s. The Riccati equation (49) is solved backward in time using the ODE45 solver of the MATLAB environment. The kinematics and dynamics components of the simulations were implemented at a much higher rate to properly capture their continuous nature. Additionally, to ensure precise evaluation of the missiles' miss distances, high resolution integration is performed when the missiles are in close proximity to the target. After the leading missile passes the target, the simulation continues to run to evaluate the performance of the second missile. In all simulations, perfect information is considered for the target.

## B. Perfect Information Sample Run Examples

Before turning to a statistical MC evaluation, first we present two sample run examples. For both examples, the missiles are guided toward the target having perfect information, i.e., without an estimator in the loop. The first missile employs a PN guidance law with  $N'_{PN} = 4$ , whereas the second missile uses OGL with  $\varepsilon = 0$ . The initial flight path angle of the target is  $\gamma_{t;0} = 0^\circ$  and the missiles are on a perfect collision triangle with the target. We consider 10 g maximum maneuverability limit for the target.

The first example considers the target performing a maximum acceleration maneuver to one side throughout

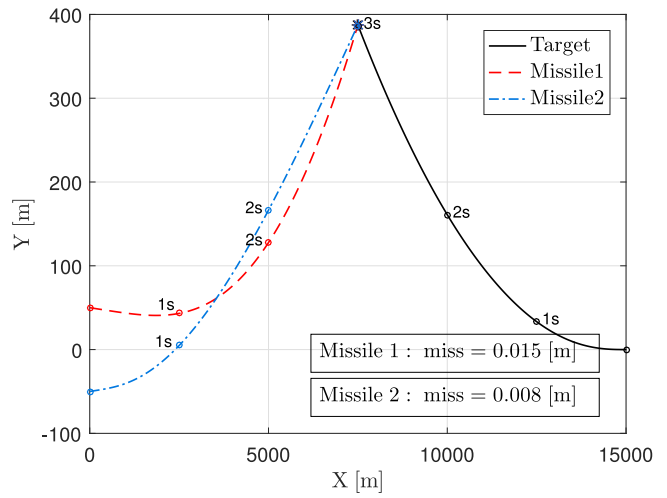


Fig. 3. Sample run planar trajectories. Target performs a 10 g maximum acceleration maneuver to one side (no blinding).

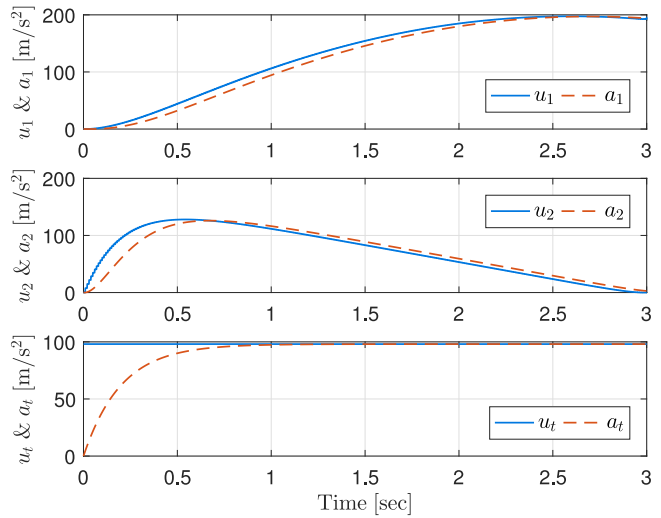


Fig. 4. Acceleration profiles of the missiles and the target. Target performs a 10 g maximum acceleration maneuver to one side (no blinding).

the entire duration of the engagement, i.e., without blinding the missiles. This scenario corresponds to the limit case of the proposed blinding-evasion guidance (52) with  $\Delta t_s$  being set to  $t^f$ , thus  $t_s^f = 0$ , meaning pure evasion only. The obtained trajectories for this scenario are shown in Fig. 3 with corresponding acceleration profiles depicted in Fig. 4. The second example considers the target employing the proposed blinding-evasion guidance strategy with the switch parameter  $\Delta t_s$  being set to 0.5 s. Fig. 5 shows the resulting trajectories, whereas Fig. 6 depicts the corresponding acceleration profile.

As expected, perfect information guidance leads to very small miss distances in both examples. However, when the blinding guidance approach is not active, the trajectories of the missiles are separated from each other most of the time, see Fig. 3. This in turn, and as will be shown in the next section, allows the missiles to make use of the triangular structure by exploiting the missiles' LOS

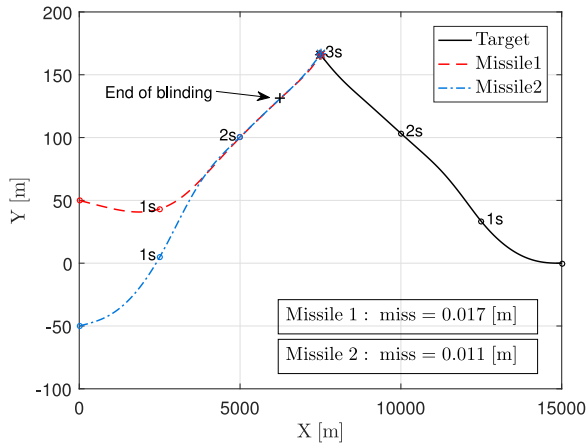


Fig. 5. Sample run planar trajectories. Target employs the proposed blinding-evasion guidance strategy with  $\Delta t_s = 0.5$  s.

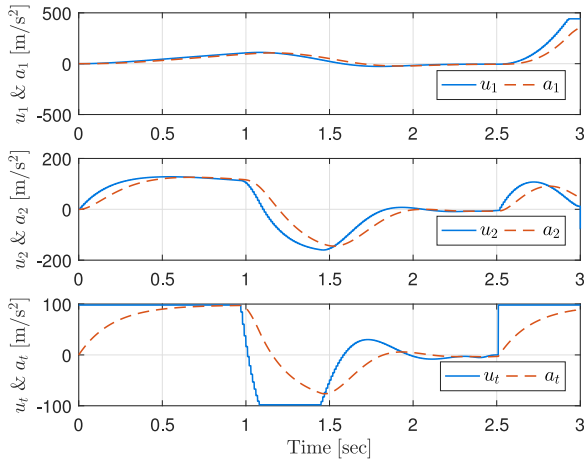


Fig. 6. Acceleration profiles of the missiles and the target. Target employs the proposed blinding-evasion guidance strategy with  $\Delta t_s = 0.5$  s.

angle measurements from different look angles. On the other hand, when the blinding guidance law of the target is active, the trajectories of the missiles are shaped such that the LOS separation angle becomes close to zero within a relatively short time, despite limited maneuver capability of the target, see Figs. 5 and 6.

### C. Pure Estimation Performance Evaluation

To evaluate the missiles' estimation performance without interfering with their guidance, again perfect information is considered to guide the missiles. The engagement geometry and missiles' guidance parameters are the same as in the previous section. Four different values of the target's switch parameter  $\Delta t_s$  are considered. For each  $\Delta t_s \in \{t^f, 1, 0.5, 0\}$ , a set of 500 MC runs is performed.

Fig. 7 presents the obtained results for the estimator associated with the first missile<sup>5</sup> in terms of the actual standard deviations of estimation errors (1-sigma values). The

<sup>5</sup>Results for the estimator associated with the second missile are omitted as the obtained results are very similar to those in Fig. 7. This comes as a consequence of both missiles processing the same measurement sequences.

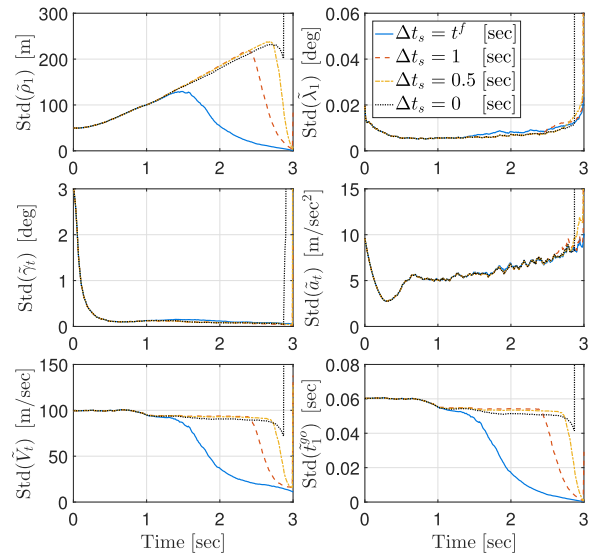


Fig. 7. Estimation performance of the first missile. Standard deviation of the state estimation errors evaluated based on 500 MC runs.

symbol  $\sim$  over the respective variables indicates the error between the true and estimated value. In addition to the five estimated states ( $\rho_1$ ,  $\lambda_1$ ,  $\gamma_1$ ,  $a_1$ , and  $V_1$ ), we also depict the accuracy of the time-to-go approximation.

In line with the discussion in Section III-D, it can be observed from Fig. 7 that the estimation accuracy of some variables deteriorates as  $\Delta t_s$  becomes smaller (meaning longer blinding), especially that of the range, speed, and time-to-go. Note that  $\Delta t_s = 0$  corresponds to another limiting case of (52), when only blinding is performed. In this case, all the estimated variables diverge near the end of the engagement.

### D. Miss Distance Evaluation

Here, we analyze the intertwined guidance-estimation performance of the missiles for different values of  $\Delta t_s$  and  $\bar{u}_t$  and when the missiles are guided toward the target using estimated states from the filters. For each value of  $\Delta t_s$  and  $\bar{u}_t$ , a set of 500 MC simulations is run. For a given MC realization, the *missile team homing performance* is characterized by the smallest of the miss distances of both missiles. The guidance law and guidance parameter of each missile are distributed uniformly. The guidance parameters are restricted to  $N' \in \{3, 4, 5\}$  for PN and APN; and  $\varepsilon \in \{10^{-3}, 10^{-6}, 0\}$  for OGL. The missiles' initial flight path angles  $\gamma_{i;0}$  are chosen such that the missiles' velocity vectors point toward the initial target location

$$\gamma_{i;0} = \sin^{-1} (V_t \sin(\gamma_{t;0} + \lambda_{i;0}) / V_i) + \lambda_{i;0}, \quad i \in \{1, 2\}$$

with a 10% uniformly distributed heading error. The initial flight path angles of the target  $\gamma_{t;0}$  are drawn from a uniform distribution on the interval  $(-15^\circ, 15^\circ)$ .

Fig. 8 shows the empirical cumulative distribution function (CDF) of the *missile team homing performance* for  $\Delta t_s(s) = \{t^f, 2, 1, 0.5, 0\}$  and  $\bar{u}_t = 10$  g. It can be observed from this figure that the best choice of the target's switching parameter  $\Delta t_s$  is 0.5 s. For larger values of  $\Delta t_s$ ,

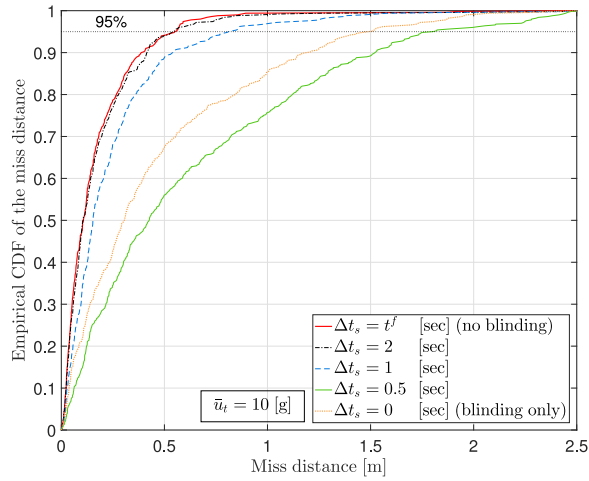


Fig. 8. CDF of the missile team miss distance for different values of  $\Delta t_s$  and  $\bar{u}_t = 10$  g.

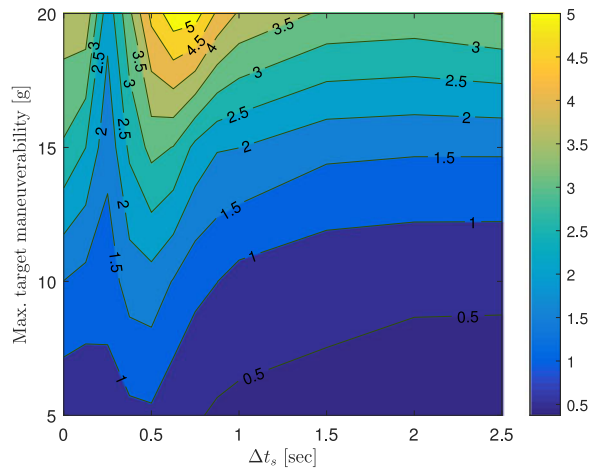


Fig. 9. Missile team miss distance (in meter) of 95% of the runs for different values of the switch parameter  $\Delta t_s$  and maximum maneuverability limit  $\bar{u}_t$ .

the homing accuracy of the missiles improves as a consequence of improved estimation performance. On the other hand, albeit the missiles are blinded throughout the engagement, i.e.,  $\Delta t_s = 0$  s, the homing accuracy of the missiles slightly improves compared to the case when  $\Delta t_s = 0.5$  s. This is expected as the target does not perform any evasion maneuver.

The homing performance of the missile team for different values of  $\bar{u}_t \in \mathcal{G}_t$  g and  $\Delta t_s$  (s)  $\in \langle 0, 2.5 \rangle$  is depicted in Fig. 9. The shades of this contour plot represent the missile team miss corresponding to the best 95% of the runs, i.e., the CDF's quantile function evaluated at 0.95 (CDFs' cross point values with the dotted horizontal line in Fig. 8). This quantity is also known as the "warhead lethality range" ensuring a 95% kill probability for the missile team. Fig. 8 suggests that for a given maximum maneuverability limit of the target  $\bar{u}_t$ , there exists an optimal value of the target's switching parameter  $\Delta t_s$  for which the missiles' homing accuracy is the worst, i.e., a value of  $\Delta t_s$ , which leads to the highest survival probability of the target.

## VI. CONCLUSION

A novel blinding-evasion guidance concept has been proposed for an aerial target to defend against a team of two homing missiles. The missiles are assumed to share their respective LOS angle measurements of the target. Provided sufficient separation between the two LOS vectors, the missiles can benefit from improved estimation accuracy of the target. Under mild requirements on the target's control authority, the proposed blinding guidance enables the target to force the two LOS vectors to coincide with each other, hence essentially "blinding" the two missiles. Subsequently, an appropriately timed evasion maneuver helps the target to increase its survivability likelihood from the blinded homing missiles.

Results from an MC simulation campaign suggest that, for a given level of target maneuverability limit, there exists an optimal timing for the switch from the blinding-only to the evasion-only strategy. For the considered parameters in this study, the optimal switching time for a target limitation of 5 g and for a target limitation of 20 g resulted to be about 0.5 s and about 0.7 s ahead of the predicted impact of the leading missile, respectively. The demonstrated capability of the proposed blinding-evasion guidance concept against two highly maneuverable homing missiles can, for a carefully selected switching time, considerably improve the target's survivability.

The limitations of this paper include the following. The employed linear guidance laws of the missiles are assumed to be perfectly known to the target; observability-enhancing guidance laws are not considered as possible maneuver strategies for the missiles; and the homing missiles rely solely on the triangulation technique to enhance observability.

## APPENDIX A CLASSICAL MISSILE GUIDANCE LAWS

The classical guidance laws of PN, APN, and OGL are normally expressed using the kinematic variables as [21]

$$u_i = N'_{i,j} \frac{Z_{i,j}}{(t_i^{\text{go}})^2 \cos(\gamma_i - \lambda_i)}, \quad j \in \{\text{PN, APN, OGL}\}$$

where  $N'_{i,j}$  is the effective navigation gain,  $Z_{i,j}$  is the missile's zero-effort-miss (ZEM) distance, and  $t_i^{\text{go}}$  is computed by

$$t_i^{\text{go}} = -\rho_i / V_{\rho i}, \quad V_{\rho i} < 0.$$

Note that, in some cases, a more accurate time-to-go estimation might be needed such as the one reported in [26] and [27].

The expression for the ZEM distance is different for each guidance law, i.e.,

$$\begin{aligned} Z_{i,\text{PN}} &= -V_{\rho i} \dot{\lambda}_i (t_i^{\text{go}})^2 \\ Z_{i,\text{APN}} &= Z_{i,\text{PN}} + \frac{1}{2} (t_i^{\text{go}})^2 a_t \cos(\gamma_t + \lambda_i) \\ Z_{i,\text{OGL}} &= Z_{i,\text{APN}} - \tau_i^2 \psi(\theta_i) a_{si} \cos(\gamma_i - \lambda_i) \end{aligned}$$

where  $\dot{\lambda}_i$  and  $V_{\rho i}$  are given by (1) and (2), respectively,  $\tau_i$  is the time constant of the  $i$ th missile, and  $\psi(\theta_i)$  is a function of the normalized time-to-go  $\theta_i = t_i^{\text{go}}/\tau_i$  given by

$$\psi(\theta_i) = \exp(-\theta_i) + \theta_i - 1.$$

The navigation gains of PN and APN are constant, whereas that of the OGL is time-varying and given by

$$N'_{i,\text{OGL}} = \frac{6\theta_i^2 \psi(\theta_i)}{3 + 6\theta_i - 6\theta_i^2 + 2\theta_i^3 - 3e^{-2\theta_i} - 12\theta_i e^{-\theta_i} + 6\varepsilon/\tau_i^3}$$

where  $\varepsilon$  represents the ratio between the weights on the control effort and the miss distance in the quadratic cost function used in the OGL formulation [28].

Assuming small deviations from the collision triangles, we have that

$$-V_{\rho i} (t_i^{\text{go}})^2 \dot{\lambda}_i \approx \xi_i + \dot{\xi}_i t_i^{\text{go}}.$$

Using this expression in the definitions of the above ZEM distances, the guidance laws of PN, APN, and OGL can be easily fitted into the linear form of (43) as follows:

### 1. PN-Guided Missile

$$K_i^1 = N'_{i,\text{PN}}/(t_i^{\text{go}})^2, \quad K_i^2 = N'_{i,\text{PN}}/t_i^{\text{go}} \\ K_i^m = \mathbf{0}, \quad K_i^t = \mathbf{0}, \quad K_i^u = \mathbf{0}.$$

### 2. APN-Guided Missile

$$K_i^1 = N'_{i,\text{APN}}/(t_i^{\text{go}})^2, \quad K_i^2 = N'_{i,\text{APN}}/t_i^{\text{go}}, \quad K_i^m = \mathbf{0} \\ K_i^t = k_t N'_{i,\text{APN}} \mathbf{C}_t/2, \quad K_i^u = k_t N'_{i,\text{APN}} \mathbf{D}_t/2.$$

### 3. OGL-Guided Missile

$$K_i^1 = N'_{i,\text{OGL}}/(t_i^{\text{go}})^2, \quad K_i^2 = N'_{i,\text{OGL}}/t_i^{\text{go}} \\ K_i^m = -k_i N'_{i,\text{OGL}} \psi(\theta_i) \mathbf{C}_i/\theta_i^2, \quad K_i^t = k_t N'_{i,\text{OGL}} \mathbf{C}_t/2 \\ K_i^u = k_t N'_{i,\text{OGL}} \mathbf{D}_t/2.$$

## APPENDIX B PARTICULAR MATRICES OF THE MATRIX EQUATION (44)

$$A_{2l}^{\circ} = \begin{bmatrix} -k_l D_1 K_1^l & \mathbf{0} \\ \mathbf{0} & -k_l D_2 K_2^l \end{bmatrix}, \quad l \in \{1, 2\} \\ A_{23}^{\circ} = \begin{bmatrix} -k_1 (\mathbf{C}_1 + D_1 \mathbf{K}_1^m) & \mathbf{0} \\ \mathbf{0} & -k_2 (\mathbf{C}_2 + D_2 \mathbf{K}_2^m) \end{bmatrix}$$

$$A_{24}^{\circ} = \begin{bmatrix} k_{t1} \mathbf{C}_t - k_1 D_1 \mathbf{K}_1^t \\ k_{t2} \mathbf{C}_t - k_2 D_2 \mathbf{K}_2^t \end{bmatrix}, \quad A_{34}^{\circ} = \begin{bmatrix} \mathbf{B}_1 \mathbf{K}_1^t \\ \mathbf{B}_2 \mathbf{K}_2^t \end{bmatrix} \\ A_{3l}^{\circ} = \begin{bmatrix} \mathbf{B}_1 \mathbf{K}_1^l & \mathbf{0} \\ \mathbf{0} & \mathbf{B}_2 \mathbf{K}_2^l \end{bmatrix}, \quad l \in \{1, 2\} \\ A_{33}^{\circ} = \begin{bmatrix} \mathbf{A}_1 + \mathbf{B}_1 \mathbf{K}_1^m & \mathbf{0} \\ \mathbf{0} & \mathbf{A}_2 + \mathbf{B}_2 \mathbf{K}_2^m \end{bmatrix} \\ A_{51}^{\circ} = [-V_{c1}^{-1} (t_1^{\text{go}})^{-2} \quad V_{c2}^{-1} (t_2^{\text{go}})^{-2}] \\ A_{52}^{\circ} = [-(V_{c1} t_1^{\text{go}})^{-1} \quad (V_{c2} t_2^{\text{go}})^{-1}] \\ \mathbf{B}_2^{\circ} = \begin{bmatrix} k_{t1} D_t - k_1 D_1 K_1^u \\ k_{t2} D_t - k_2 D_2 K_2^u \end{bmatrix}, \quad \mathbf{B}_3^{\circ} = \begin{bmatrix} \mathbf{B}_1 K_1^u \\ \mathbf{B}_2 K_2^u \end{bmatrix}.$$

## REFERENCES

- [1] B. A. Jackson, D. R. Frelinger, M. J. Lostumbo, and R. W. Button *Evaluating Novel Threats to the Homeland: Unmanned Aerial Vehicles and Cruise Missiles*, vol. 626. Santa Monica, CA, USA: RAND Corporation, 2008.
- [2] S. Balakrishnan, A. Tsourdos, and B. White *Advances in Missile Guidance, Control, and Estimation*. Boca Raton, FL, USA: CRC Press, 2012.
- [3] V. Shaferman and T. Shima Cooperative multiple-model adaptive guidance for an aircraft defending missile *J. Guid., Control, Dyn.*, vol. 33, no. 6, pp. 1801–1813, 2010.
- [4] T. Shima Optimal cooperative pursuit and evasion strategies against a homing missile *J. Guid., Control, Dyn.*, vol. 34, no. 2, pp. 414–425, 2011.
- [5] A. Ratnoo and T. Shima Line-of-sight interceptor guidance for defending an aircraft *J. Guid., Control, Dyn.*, vol. 34, no. 2, pp. 522–532, 2011.
- [6] R. Fonod and T. Shima Estimation enhancement by cooperatively imposing relative intercept angles *J. Guid., Control, Dyn.*, vol. 40, no. 7, pp. 1711–1725, 2017.
- [7] J. L. Speyer An adaptive terminal guidance scheme based on an exponential cost criterion with application to homing missile guidance *IEEE Trans. Autom. Control*, vol. AC-21, no. 3, pp. 371–375, Jun. 1976.
- [8] R. Fonod and T. Shima Multiple model adaptive evasion against a homing missile *J. Guid., Control, Dyn.*, vol. 39, no. 7, pp. 1578–1592, 2016.
- [9] V. Turetsky and T. Shima Target evasion from a missile performing multiple switches in guidance law *J. Guid., Control, Dyn.*, vol. 39, no. 10, pp. 2364–2373, 2016.
- [10] J. L. Speyer, D. G. Hull, S. Larson, and C. Tseng Estimation enhancement by trajectory modulation for homing missiles *J. Guid., Control, Dyn.*, vol. 7, no. 2, pp. 167–174, 1984.
- [11] D. Hull, J. Speyer, and C. Tseng Maximum-information guidance for homing missiles *J. Guid., Control, Dyn.*, vol. 8, no. 4, pp. 494–497, 1985.
- [12] T. L. Song and T. Y. Um Practical guidance for homing missiles with bearings-only measurements *IEEE Trans. Aerosp. Electron. Syst.*, vol. 32, no. 1, pp. 434–443, Jan. 1996.
- [13] M.-G. Seo and M.-J. Tahk Observability analysis and enhancement of radome aberration estimation with line-of-sight angle-only measurement *IEEE Trans. Aerosp. Electron. Syst.*, vol. 51, no. 4, pp. 3321–3331, Oct. 2015.

- [14] T.-H. Kim, C.-H. Lee, and M.-J. Tahk  
Time-to-go polynomial guidance with trajectory modulation for observability enhancement  
*IEEE Trans. Aerosp. Electron. Syst.*, vol. 49, no. 1, pp. 55–73, Jan. 2013.
- [15] S. Battistini and T. Shima  
Differential games missile guidance with bearings-only measurements  
*IEEE Trans. Aerosp. Electron. Syst.*, vol. 50, no. 4, pp. 2906–2915, Oct. 2014.
- [16] V. Shaferman and Y. Oshman  
Cooperative interception in a multi-missile engagement  
In *Proc. AIAA Guid., Navig., Control Conf.*, Chicago, IL, Aug. 2009, pp. 10–13.
- [17] Y. Liu, N. Qi, and J. Shan  
Cooperative interception with double-line-of-sight-measuring  
In *Proc. AIAA Guid., Navig., Control Conf.* Boston, MA, USA: AIAA, 2013.
- [18] V. Shaferman and Y. Oshman  
Stochastic cooperative interception using information sharing based on engagement staggering  
*J. Guid., Control, Dyn.*, vol. 39, no. 9, pp. 2127–2141, 2016.
- [19] R. A. Singer  
Estimating optimal tracking filter performance for manned maneuvering targets  
*IEEE Trans. Aerosp. Electron. Syst.*, vol. AES-6, no. 4, pp. 473–483, Jul. 1970.
- [20] Y. Bar-Shalom, X. R. Li, and T. Kirubarajan  
*Estimation With Applications to Tracking and Navigation: Theory Algorithms and Software*. New York, NY, USA: Wiley, 2001.
- [21] P. Zarchan  
*Tactical and Strategic Missile Guidance* (Progress in Astronautics and Aeronautics), vol. 199. Reston, VA, USA: AIAA, 2002.
- [22] E. Kreindler and P. Sarachik  
On the concepts of controllability and observability of linear systems  
*IEEE Trans. Autom. Control*, vol. AC-9, no. 2, pp. 129–136, Apr. 1964.
- [23] E. A. Bryson and C. Y. Ho  
*Applied Optimal Control*. Waltham, MA, USA: Blaisdell, 1969.
- [24] J. Ben-Asher, E. M. Cliff, and H. J. Kelley  
Optimal evasion with a path-angle constraint and against two pursuers  
*J. Guid., Control, Dyn.*, vol. 11, no. 4, pp. 300–304, 1988.
- [25] A. Jameson, W. Schmidt, and E. Turkel  
Numerical solution of the Euler equations by finite volume methods using Runge Kutta time stepping schemes  
In *Proc. AIAA 14th Fluid Plasma Dyn. Conf.*, Palo Alto, CA, USA, 1981.
- [26] C.-K. Ryoo, H. Cho, and M.-J. Tahk  
Time-to-go weighted optimal guidance with impact angle constraints  
*IEEE Trans. Control Syst. Technol.*, vol. 14, no. 3, pp. 483–492, May 2006.
- [27] N. Dhananjay and D. Ghose  
Accurate time-to-go estimation for proportional navigation guidance  
*J. Guid., Control, Dyn.*, vol. 37, no. 4, pp. 1378–1383, 2014.
- [28] J. Z. Ben-Asher and I. Yaesh  
*Advances in Missile Guidance Theory* (Progress in Astronautics and Aeronautics), vol. 180. Reston, VA, USA: AIAA, 1971.



**Robert Fonod** (S'10–M'15) received the Ph.D. degree in automation from the University of Bordeaux, Talence, France, in 2014.

He is currently a Postdoctoral Research Fellow in the Department of Aerospace Engineering, Technion - Israel Institute of Technology, Haifa, Israel. His current research interests include the area of guidance and estimation of aerial vehicles, bearings-only target tracking, and stability of nonlinear filters.



**Tal Shima** (SM'05) received the Ph.D. degree from the Technion - Israel Institute of Technology, Haifa, Israel, in 2001.

He is currently an Associate Professor in the Department of Aerospace Engineering, Technion. His current research interests include the area of guidance of vehicles, in particular missiles and unmanned aircraft, operating individually or as a team. He is an Associate Fellow of AIAA.